

# **Modelling of Entrainment and Development of an Improved Debris Mobility Modelling Program “2d-DMM (Version 3.0)”**

**GEO Report No. 367**

**E.K.L. Wong, R.P.H. Law & I. Li**

**Geotechnical Engineering Office  
Civil Engineering and Development Department  
The Government of the Hong Kong  
Special Administrative Region**

[Blank Page]

# **Modelling of Entrainment and Development of an Improved Debris Mobility Modelling Program “2d-DMM (Version 3.0)”**

**GEO Report No. 367**

**E.K.L. Wong, R.P.H. Law & I. Li**

**This report was originally produced in December 2020  
as GEO Technical Note No. TN 3/2020**

© The Government of the Hong Kong Special Administrative Region

First published, February, 2024

Prepared by:

Geotechnical Engineering Office,  
Civil Engineering and Development Department,  
Civil Engineering and Development Building,  
101 Princess Margaret Road,  
Homantin, Kowloon,  
Hong Kong.

## Preface

In keeping with our policy of releasing information which may be of general interest to the geotechnical profession and the public, we make available selected internal reports in a series of publications termed the GEO Report series. The GEO Reports can be downloaded from the website of the Civil Engineering and Development Department (<http://www.cedd.gov.hk>) on the Internet.



Raymond W M Cheung  
Head, Geotechnical Engineering Office  
February 2024

## Foreword

The dynamics of landslide debris mobility can be modified substantially by entrainment during the run-out process. Accurate modelling of entrainment is essential in landslide debris mobility analysis for the assessment of landslide hazard. The present technical study comprising a review of the state-of-the-art theory and methodologies of entrainment modelling was thus initiated. As part of this study, the in-house debris mobility program 2d-DMM was enhanced by incorporating a physically based entrainment model, and field mapping records of mobile debris flows triggered by the 7 June 2008 rainstorm were re-visited to obtain useful insights in the entrainment depth that could occur in extreme events. The study was undertaken by Mr E.K.L. Wong, Dr R.P.H. Law and Mr I. Li under the supervision of Dr J.S.H. Kwan. The Drafting Unit of the Standards and Testing Division assisted in formatting this report. All contributions are gratefully acknowledged.



T.K.C. Wong  
Chief Geotechnical Engineer/Standards and Testing

## **Abstract**

This GEO Report documents a literature review of the latest development in entrainment calculation, and the improvements made to the Geotechnical Engineering Office's in-house debris mobility program 2d-DMM with inclusion of a physically based entrainment model. The process of verification of the improved 2d-DMM is also documented. As part of this study, field mapping records of mobile debris flows triggered by the 7 June 2008 rainstorm have been re-visited. Insights into the entrainment depth that could occur in extreme events are also presented in this report.

## Contents

	Page No.
Title Page	1
Preface	3
Foreword	4
Abstract	5
Contents	6
List of Tables	7
List of Figures	8
1 Background	9
2 Literature Review	9
3 Improvements to Computer Program “2d-DMM”	12
4 Validation of 2d-DMM (Version 3.0)	13
4.1 Comparison with Simplified Analytical Lumped-mass Solutions	13
4.2 Comparison with DAN-W	15
4.2.1 Channel of Constant Width	16
4.2.1.1 Friction Model	16
4.2.1.2 Voellmy Model	17
4.2.2 Channel of Variable Width	18
4.3 Simulation of Yu Tung Road Debris Flow	19
5 Entrainment Depth of Debris Flow Events in Hong Kong	21
6 Conclusion	27
7 References	27



**List of Tables**

Table No.		Page No.
4.1	Comparison between 2d-DMM and DAN-W Results Using Friction Model	16
4.2	Comparison between 2d-DMM and DAN-W Results Using Voellmy Model	17
4.3	Comparison between 2d-DMM and DAN-W Results for Channel of Variable Width	18
4.4	Entrainment Depths as Determined from Mapping Record	19
5.1	Debris Flow Events with Greatest Entrained Volume under 2015 Study	22

## List of Figures

Figure No.		Page No.
4.1	Lumped-mass Model	14
4.2	Infinite Slope Model Used for Calibration against Analytical Solution	14
4.3	Comparison between Analytical and 2d-DMM Results	15
4.4	Ground Profile Used for Validation against DAN-W	16
4.5	Velocity Profile from 2d-DMM and DAN-W Using Friction Model	17
4.6	Velocity Profile from 2d-DMM and DAN-W Using Voellmy Model	17
4.7	Channel Width Used in Validation between 2d-DMM and DAN-W	18
4.8	Velocity Profile from 2d-DMM and DAN-W	19
4.9	Debris Velocity along Yu Tung Road Debris Flow	21
5.1	Locations of Debris Flow Events Considered	22
5.2	Distribution of Entrainment Depth in Selected Debris Flow Events	23
5.3	Distribution of Entrainment Depth with Length of Mapping Section	23
5.4	Distribution of Entrainment Depth with Slope Gradient	24
5.5	Distribution of Entrainment Depth with Catchment Size	25
5.6	Distribution of Entrainment Depth with Catchment Shape	25
5.7	Distribution of Entrainment Depth with Drainage Density	26

## 1 Background

is The 2d-DMM (Version 2.0) (GEO, 2015; Law & Ko, 2015) is a computer program for debris mobility analysis developed in-house by the Geotechnical Engineering Office (GEO), in which the volume of entrainment is calculated based on a rate of volumetric increment with time (in  $\text{m}^3/\text{s}$ ) specified by users. In 2019, the GEO initiated a study for enhancing the entrainment modelling in 2d-DMM. This study includes a literature review of the latest developments in entrainment calculation, coding of a suitable entrainment calculation methodology and verification of the coding and documentation. This report presents the findings of this study.

## 2 Literature Review

There are many computer programs for debris mobility analysis. Kwan et al. (2021) reported the development of debris mobility models in Hong Kong. A suite of numerical tools with different levels of sophistication have been developed to meet the need of landslide risk management. Examples are two-dimensional debris mobility models 2d-DMM (Kwan & Sun, 2006) and various three-dimensional models: 3d-DMM formulated using different numerical techniques including the particle-in-cell method (Kwan & Sun, 2007), the smoothed particle hydrodynamics method (Law et al., 2017) and the arbitrary Lagrangian-Eulerian method (Koo et al., 2018). Together with other numerical tools, such as DAN-W (Hung, 1995) and DAN3D (McDougall & Hung, 2004), back analyses of historical landslides have been conducted to validate the prediction capability of the debris mobility models (e.g. Hung et al., 2007; Pastor et al., 2018). These tools have been shown to produce results consistent with site observations. Some of the numerical models have also been applied in routine engineering practice for forward prediction purposes (Kwan et al., 2021)

Meanwhile, there have been relatively few studies on entrainment modelling. In practice, simplifications by assessing a constant active landslide volume during the debris run-out process are often adopted. This kind of analysis neglects the physical role of surficial materials. However, the entrainment of these materials could increase the debris volume, alter the composition, and ultimately enhance the mobility of the landslide (McDougall & Hung, 2005).

An early 2D model in Lagrangian framework was presented by Hung (1995) in the development of DAN-W. The effect of deposition or entrainment in DAN-W is modelled by changing the volume of the flowing debris at each time step by a prescribed amount proportional to the distance travelled. The rate of erosion increases with the flow depth, resulting in a depth-proportional distribution of entrained material and natural exponential growth of the landslide with displacement. Although largely empirical, this method has a physical basis where the changes in stress conditions leading to failure within the path material can be related to changes in the total bed-normal stress and therefore the flow depth (McDougall & Hung, 2005).

Further development in the incorporation of entrainment into mobility modelling was made by McDougall & Hung (2004) in association with the development of DAN3D, an extension to DAN. In DAN3D's formulation, the effect of entrainment is expressed as a "bed-erosion" term ( $E_t = \partial b / \partial t$ ), or known as "erosion velocity" as defined by

Takahashi (1991).  $E_t$  is then incorporated into the governing equation of motion, i.e. the depth averaged mass balance equation (Equation 2.1) and depth averaged momentum balance equations (Equations 2.2 and 2.3).

$$\frac{\partial h}{\partial t} + h \left( \frac{\partial v_x}{\partial x} + \frac{\partial v_y}{\partial y} \right) = \frac{\partial b}{\partial t} \dots\dots\dots (2.1)$$

where  $h$  = flow depth  
 $v$  = flow velocity  
 $b$  = bed-normal erosion depth.

$$\rho h \frac{\partial v_x}{\partial t} = \rho h g_x + k_x \sigma_z \left( -\frac{\partial h}{\partial x} \right) + k_{yx} \sigma_z \left( -\frac{\partial h}{\partial y} \right) + \tau_{zx} - \rho v_x \frac{\partial b}{\partial t} \dots\dots\dots (2.2)$$

$$\rho h \frac{\partial v_y}{\partial t} = \rho h g_y + k_y \sigma_z \left( -\frac{\partial h}{\partial y} \right) + k_{xy} \sigma_z \left( -\frac{\partial h}{\partial x} \right) + \tau_{zy} - \rho v_y \frac{\partial b}{\partial t} \dots\dots\dots (2.3)$$

where  $\rho$  = density of both landslide and path materials  
 $g$  = gravitational acceleration  
 $\tau$  = basal shear stress  
 $k_x, k_{yx}, k_y, k_{xy}$  = lateral stress coefficients normalised by bed-normal stress  $\sigma_z$ .

Therefore, this results in a velocity-dependent inertial resistance, which is additional to the basal shear resistance, consistent with Perla et al. (1980)'s formulation.

The determination of erosion velocity  $E_t$  is explained in detail by McDougall & Hungr (2005). DAN3D adopted an empirical approach to determine the erosion rate which is similar to DAN by introducing an “entrainment parameter”  $E$ . The entrainment parameter  $E$  is regarded as the growth rate representing the bed-normal depth eroded per unit flow depth per unit displacement. This displacement-dependent growth rate has a unit of  $m^{-1}$ . By relating  $E_t$  to  $h$  and  $v$ , the following expression is obtained:

$$E_t = \frac{\partial b}{\partial t} = E h v \dots\dots\dots (2.4)$$

While being a simple approach, the main limitation of using this parameter  $E$  is the assumption regarding the distribution of entrained material along the passing landslide as this is usually difficult to justify. Adjustment of  $E$  by trial and error may be required.

As a preliminary assessment, McDougall & Hungr (2005) recommended the parameter  $E$  to be computed by assuming an average growth rate with displacement in natural exponential manner as follows:

$$\bar{E} = \frac{\ln(V_f/V_o)}{\bar{S}} \dots\dots\dots (2.5)$$

where  $V_0$  = estimated total volume entering the zone  
 $V_f$  = estimated total volume existing the zone  
 $S$  = approximate average path length of the zone

Pirulli & Pastor (2012) reviewed literatures published between 1963 to 2008 regarding entrainment rate formulae for different types of flow. They summarised the formulae and found that many relate the entrainment rate to flow velocity and / or to flow depth, including the form proposed by McDougall & Hungr (2005). Pirulli & Pastor (2012) reported that empirical-type formulae are the most frequently used (12 out of 15 of the publications reviewed derived formulae using empirical laws). The entrainment rate formula by McDougall & Hungr (2005) also falls within this category. Compared with other empirical methods, their method is mainly used for back-analysis and requires one user-specified parameter, (i.e.  $E$  in Equation 2.4), which is usually obtained through calibration. However, given sufficient geological information for describing other events of similar nature, Pirulli & Pastor (2012) commented that the method proposed by McDougall & Hungr (2005) is simple yet effective.

Another documentation and review on entrainment modelling was carried out by Iverson & Ouyang (2015) on literatures published between 1987 to 2014. They critically evaluated modelling methods of erosive mass flows by comprehensively deriving depth-integrated mass and momentum conservation equations for a two-layer model that can exchange mass and momentum with adjacent layers. From the derivation, they reported that many existing entrainment rate formulae lack explicit dependence on boundary tractions, including the method proposed by McDougall & Hungr (2005) (i.e. Equations (2.4) and (2.5)). However, inclusion of boundary traction into erosion rate formula must be accompanied by knowledge of the constitutive behaviour of the bed and flow materials to account for the shear and normal tractions at the eroding surfaces. As mentioned by Iverson & Ouyang (2015), a critical issue concerns the identification of the magnitude and location of basal slip in complicated sediment beds that contain natural grains with varying shapes and sizes.

Apart from the above continuum-based formulation, a coupled computational fluid dynamics and discrete element method (CDF-DEM) was reported by Kong et al. (2018) to simulate a debris flow as a mixture of a gap-graded particle system and viscous fluid. The erodible bed was simulated by bonded particles and the erosion criterion depended on the debonding thresholds. It however remains a preliminary pilot study and further development on systematic calibration and verification procedures is needed as commented by Kong et al. (2018).

In a more recent review on the modelling of flowslides and debris, Cuomo (2020) also reported that analytical bed entrainment analysis requires a proper constitutive model for the behaviour of the interface between the propagating landslide and the ground surface. Cuomo (2020) also reported that there are very few analytical models for bed entrainment in the current literature, and therefore their application to real case histories is still limited.

Based on the above review, McDougall & Hungr (2005)'s method was found to be widely adopted (Cuomo et al., 2014; Iverson & Ouyang, 2015; Shen et al., 2018; Pirulli et al., 2018; Cuomo, 2020) owing to its simplicity and ability to produce results consistent with field observation through calibration. The calculation of erosion velocity based on overburden and debris velocity also explains some physics behind the process.

### 3 Improvements to Computer Program “2d-DMM”

The entrainment calculation in 2d-DMM (Version 2.0) (GEO, 2015) essentially follows the calculation adopted in 2d-DMM (Version 1.0). According to the user manual of 2d-DMM (Version 1.0), the change of landslide volume along the flow path due to entrainment is simulated by specifying the “channel yield rate”, which is defined as the volume entrained per unit time and similar to the formulation in Hungr & Evans (1997). Users are required to determine the entrainment rate by trial-and-error such that the entrained volume matches that suggested in geological mapping or hazard assessments.

Based on the review in Section 2, considering the complex nature and mechanisms involved in material entrainment with limited application using full analytical approach, it is considered that a semi-empirical approach with physical basis that relates entrainment rate to flow depth and flow velocity remains more favourable at this stage. The entrainment modelling in the enhanced version of 2d-DMM (i.e. Version 3.0) will incorporate a semi-empirical method similar to McDougall & Hungr (2005) owing to its simplicity and ability to produce reliable results. Therefore, in 2d-DMM (Version 3.0), the following entrainment calculation method is adopted in which the bed erosion rate  $\partial b/\partial t$  is related to the flow depth  $h$  and velocity  $v$  via an entrainment parameter  $E$ :

$$\rho h \frac{\partial v}{\partial t} = \rho h g \sin \alpha + k_x \sigma_z \left( -\frac{\partial h}{\partial x} \right) + \tau_x - \rho v \frac{\partial b}{\partial t} \dots\dots\dots (3.1)$$

$$\partial b/\partial t = E h v \dots\dots\dots (3.2)$$

where  $\alpha$  = slope inclination.

After rearranging, the volume change due to entrainment can be related to the initial debris volume and the distance travelled by the debris along the channel section:

$$\begin{aligned} \Delta V_i &= (\partial b/\partial t) A_i \Delta t \\ &= (\partial b/\partial t) A_i (\Delta s_i / v_i) \\ &= E_i h A_i \Delta s_i \\ &= E_i V_i \Delta s_i \dots\dots\dots (3.3) \end{aligned}$$

where  $\Delta V_i$  = volume change in debris block  $i$  due to entrainment  
 $A_i$  = basal area of debris block  $i$   
 $v_i$  = velocity of debris block  $i$   
 $\Delta s_i$  = displacement of debris block  $i$ .

Notably, integrating Equation 3.3 would give Equation 2.5 proposed by McDougall & Hungr (2005).

In the new version of 2d-DMM (i.e. Version 3.0), users are allowed to specify the entrainment depth  $d_k$  at each segment along the flow path. The calculation does not consider entrainment arising from the side slopes of the debris run-out channel and only applies to rectangular debris block analysis. The volume growth rate for each segment  $E_k$  is then determined as follows:

$$E_k = \frac{d_k B_k}{V_k} \dots\dots\dots (3.4)$$

It follows that

$$V_k = V_{k-1} + E_k V_{k-1} \Delta x_k \dots\dots\dots (3.5)$$

where  $d_k$  = entrainment depth within  $k^{\text{th}}$  segment  
 $B_k$  = base width of landslide trail within  $k^{\text{th}}$  segment  
 $V_k$  = volume of landslide debris after passing through  $k^{\text{th}}$  segment  
 $\Delta x_k$  = length of  $k^{\text{th}}$  flow path segment.

In other words, the value of  $E$  for each flow path segment is estimated based on the input value of  $d_i$  before the time marching calculation commences. It should be noted that the total entrainment volume estimated from geological mapping or hazard assessments may not be equal to the simulated final entrainment volume. This is because a debris block may stop without passing through a channel segment for which an entrainment depth  $d_i$  has been specified.

#### 4 Validation of 2d-DMM (Version 3.0)

##### 4.1 Comparison with Simplified Analytical Lumped-mass Solutions

The 2d-DMM results were compared with an analytical solution with a simple frictional lumped-mass on an infinite slope as shown in Figures 4.1 and 4.2. The landslide trail modelled has a width of 5 m and gradient of 20°. An entrainment depth of 0.2 m was modelled along an arbitrary section of the channel of length  $L$ . The initial horizontal length of the landslide source was assumed to be 10 m in 2d-DMM.

As shown in Figure 4.3, the acceleration of the debris blocks in 2d-DMM is consistent with that of the lumped mass. The volume entrained is within 2% of the value in the lumped-mass model.

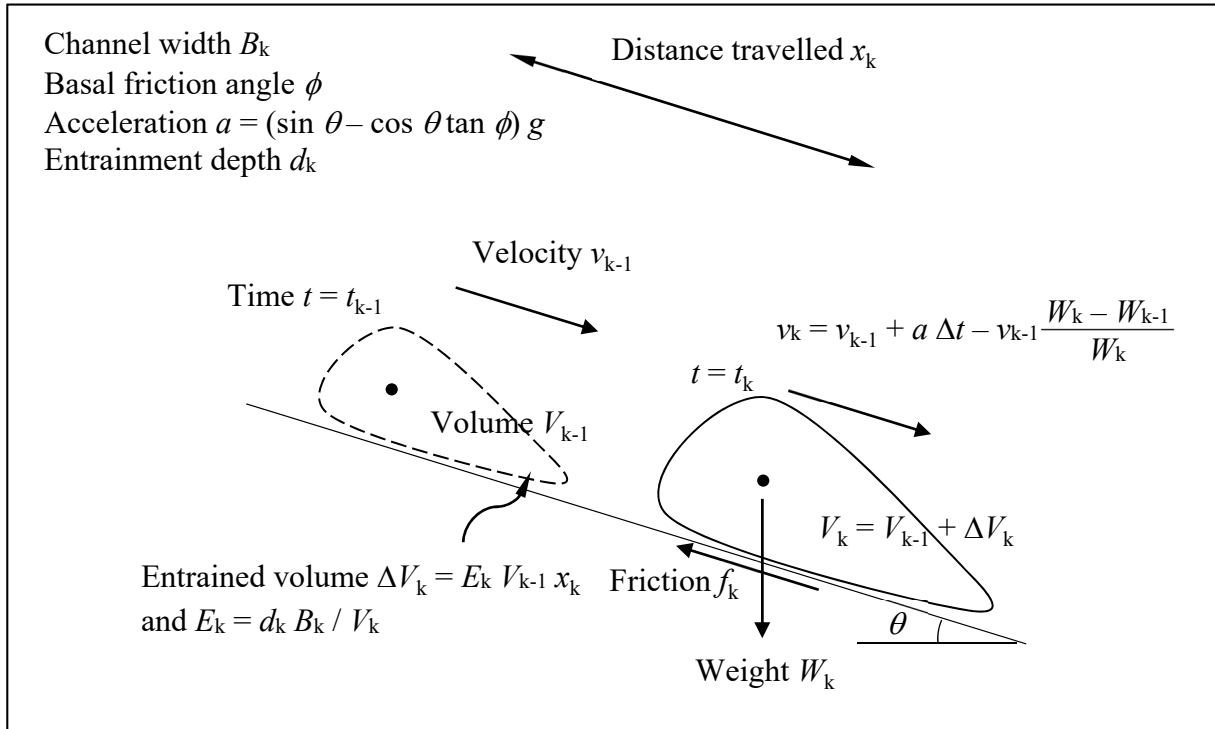


Figure 4.1 Lumped-mass Model

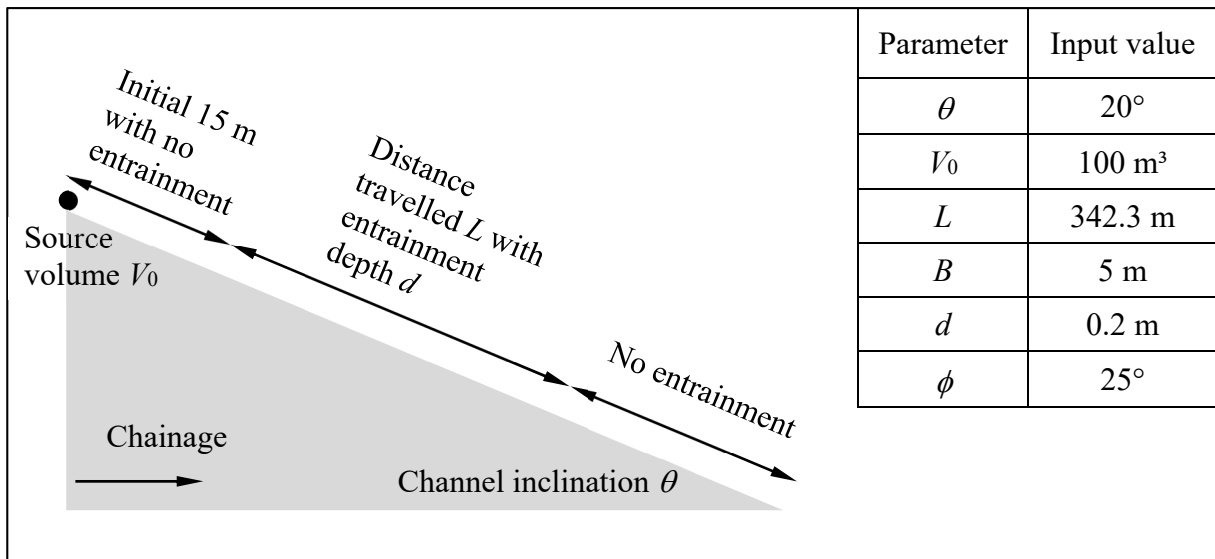
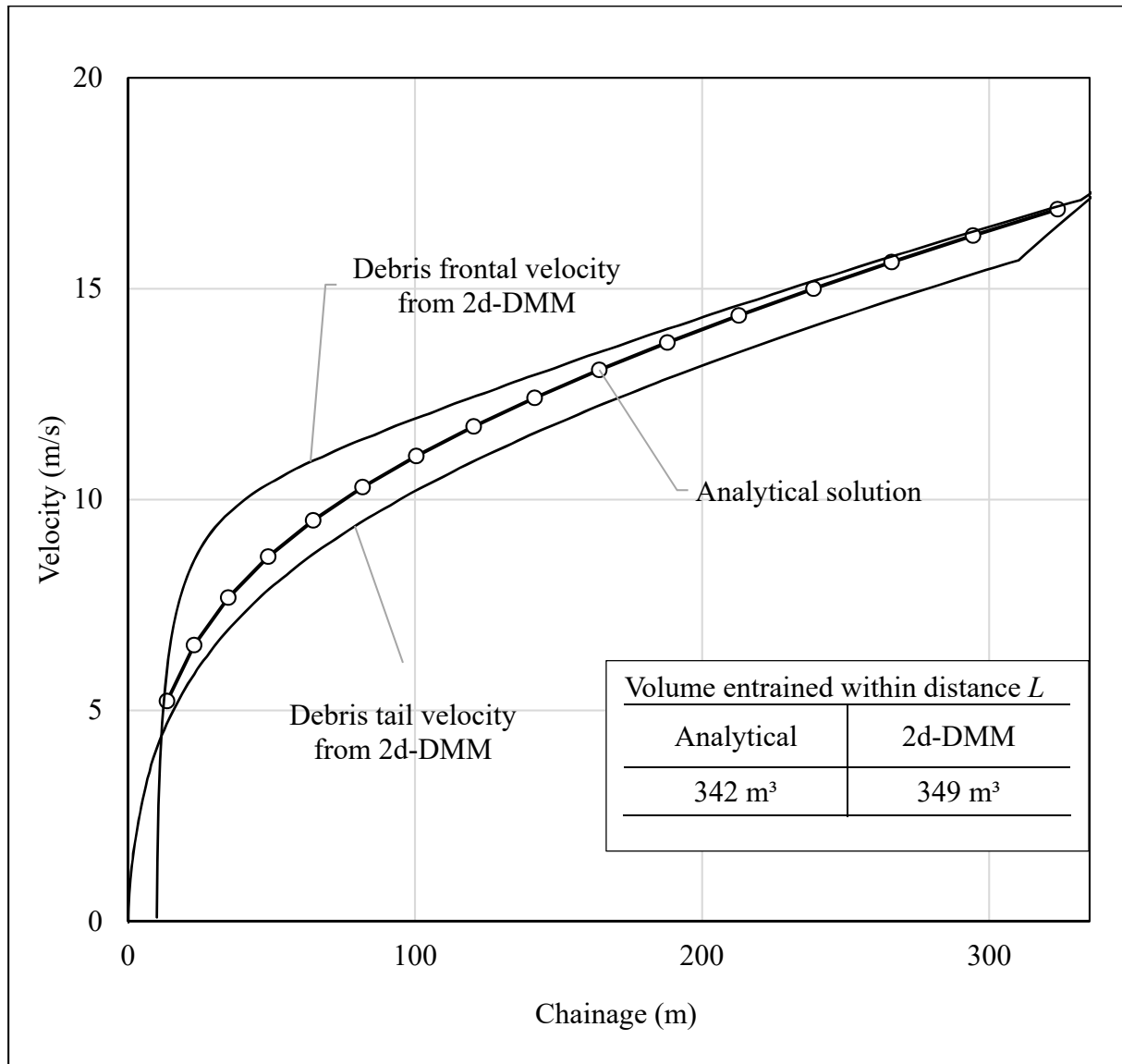


Figure 4.2 Infinite Slope Model Used for Calibration against Analytical Solution





**Figure 4.3 Comparison between Analytical and 2d-DMM Results**

#### 4.2 Comparison with DAN-W

In this section, results from 2d-DMM (Version 3.0) are compared with those from DAN-W (Release 10) (Hung, 2010), which is a similar computer program pre-accepted by the Geotechnical Engineering Office and the Buildings Department for the analysis of post-failure debris mobility.

The run-out path used in this section follows the profile of the Shek Pik “2” debris flow event (McMackin & Dee, 2008a) as shown in Figure 4.4.

DAN-W allows the user to specify the entrainment depth as a debris material property, instead of as a channel property. For simplicity, an arbitrary constant entrainment depth of 0.1 m was assumed throughout the channel. A source volume of 1,000 m<sup>3</sup> was modelled.

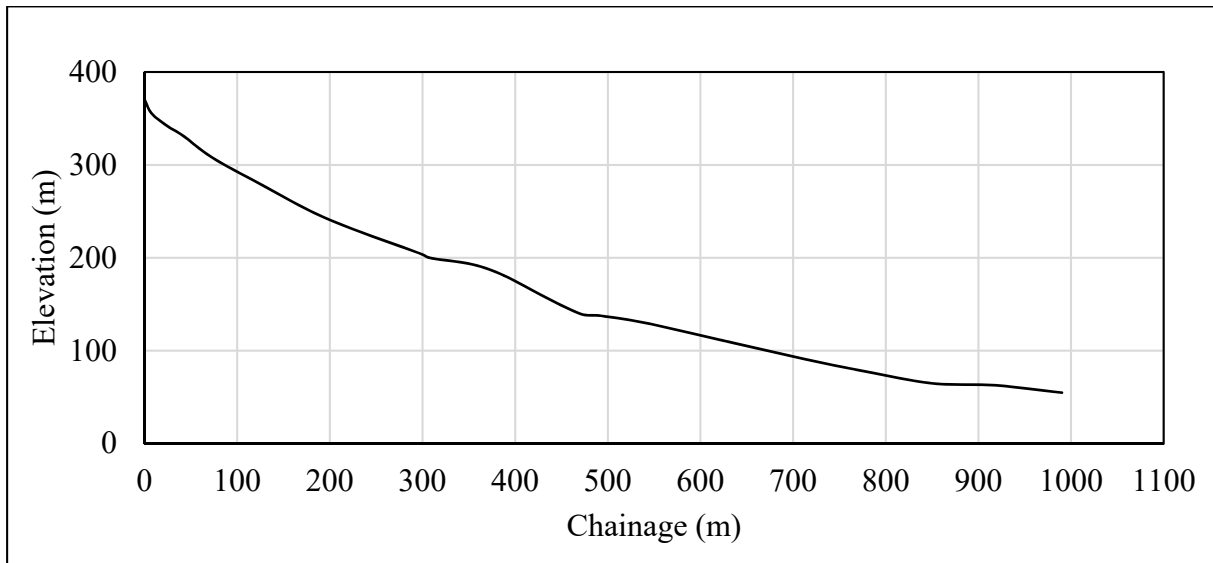


**Figure 4.4 Ground Profile Used for Validation against DAN-W**

#### 4.2.1 Channel of Constant Width

A 10 m wide rectangular channel was used. The debris density was taken as 2,200 kg/m<sup>3</sup>. Values of  $K_a$ ,  $K_p$  and  $K_0$  were assumed to be 0.8, 2.5 and 1.0 respectively. A source volume of 1,000 m<sup>3</sup> was simulated.

Two simulations involving the Friction Model and the Voellmy Model respectively were conducted. A comparison of the results from 2d-DMM and DAN-W is presented in the following section.

##### 4.2.1.1 Friction Model

The apparent basal friction angle  $\phi_a$  was taken as 20°. The total volume entrained and the debris run-out distance calculated by 2d-DMM and DAN-W are comparable (Table 4.1, Figure 4.5).

**Table 4.1 Comparison between 2d-DMM and DAN-W Results Using Friction Model**

Program	2d-DMM	DAN-W
Total volume entrained	596 m <sup>3</sup>	565 m <sup>3</sup>
Run-out distance	666 m	643 m

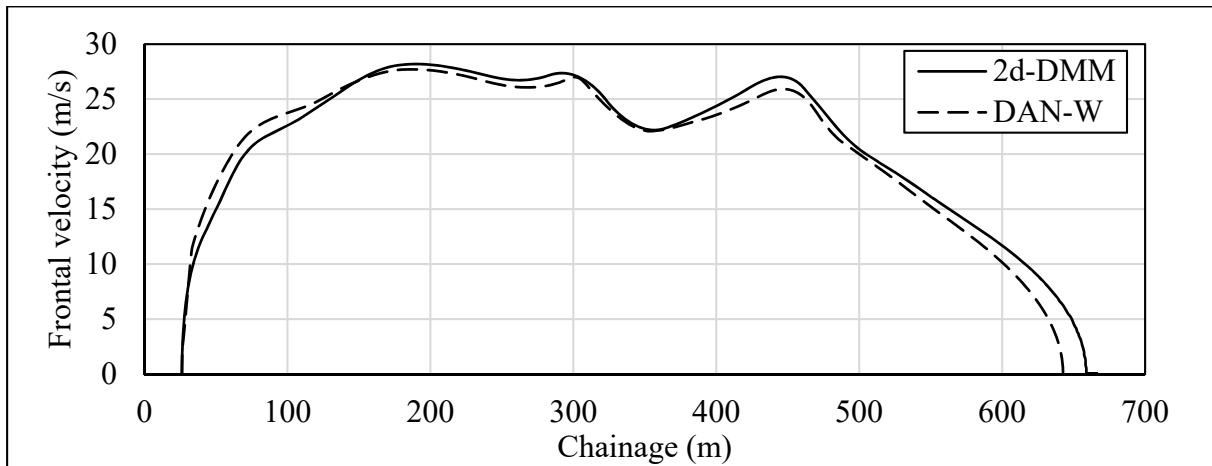


**Figure 4.5 Velocity Profile from 2d-DMM and DAN-W Using Friction Model**

#### 4.2.1.2 Voellmy Model

The apparent basal friction angle  $\phi_a$  and the Voellmy coefficient  $\xi$  were taken as  $8^\circ$  and  $500 \text{ m/s}^2$  respectively. The total volume entrained and the debris run-out distance are comparable between 2d-DMM and DAN-W (Table 4.2, Figure 4.6).

**Table 4.2 Comparison between 2d-DMM and DAN-W Results Using Voellmy Model**

Program	2d-DMM	DAN-W
Total volume entrained	1739 m <sup>3</sup>	1819 m <sup>3</sup>
Run-out distance	877 m	885 m

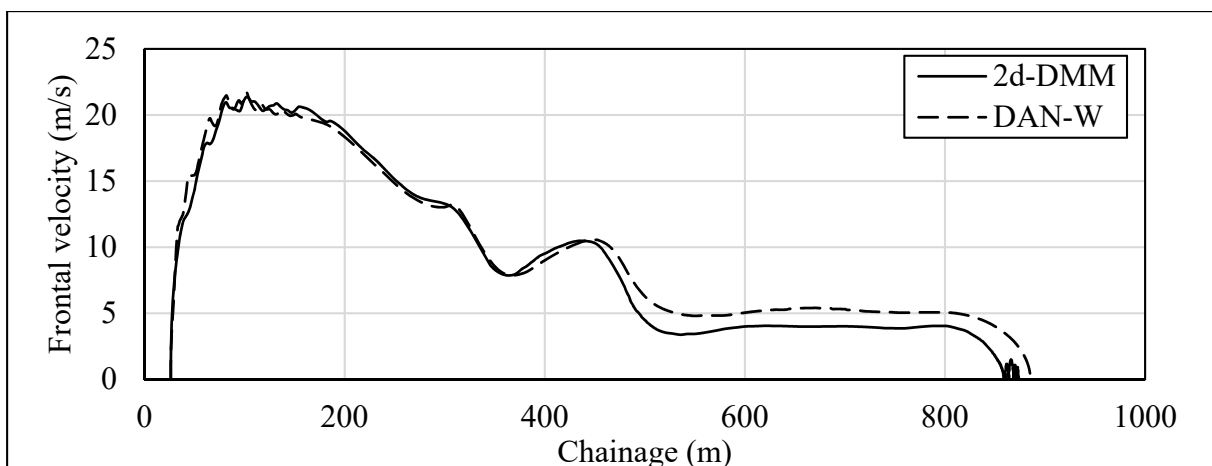


**Figure 4.6 Velocity Profile from 2d-DMM and DAN-W Using Voellmy Model<sup>1</sup>**

<sup>1</sup> The “jump” at the end of the velocity profile is a simulation artefact, resulting from the displacement of the debris block at the debris front by the debris travelling from behind.

### 4.2.2 Channel of Variable Width

The channel geometry of the Shek Pik “2” debris flow event, including the channel width determined from field geological mapping (Figure 4.7), was used in the comparison. The channel width varies between 10 m and 40 m along the channel. An arbitrary constant entrainment depth of 0.1 m was assumed throughout the whole length of the landslide trail. The apparent basal friction angle  $\phi_a$  and the Voellmy coefficient  $\xi$  were taken as  $8^\circ$  and  $500 \text{ m/s}^2$  respectively. Typical values of debris density and coefficients of lateral earth pressure were assumed as in Section 4.2.1 above.

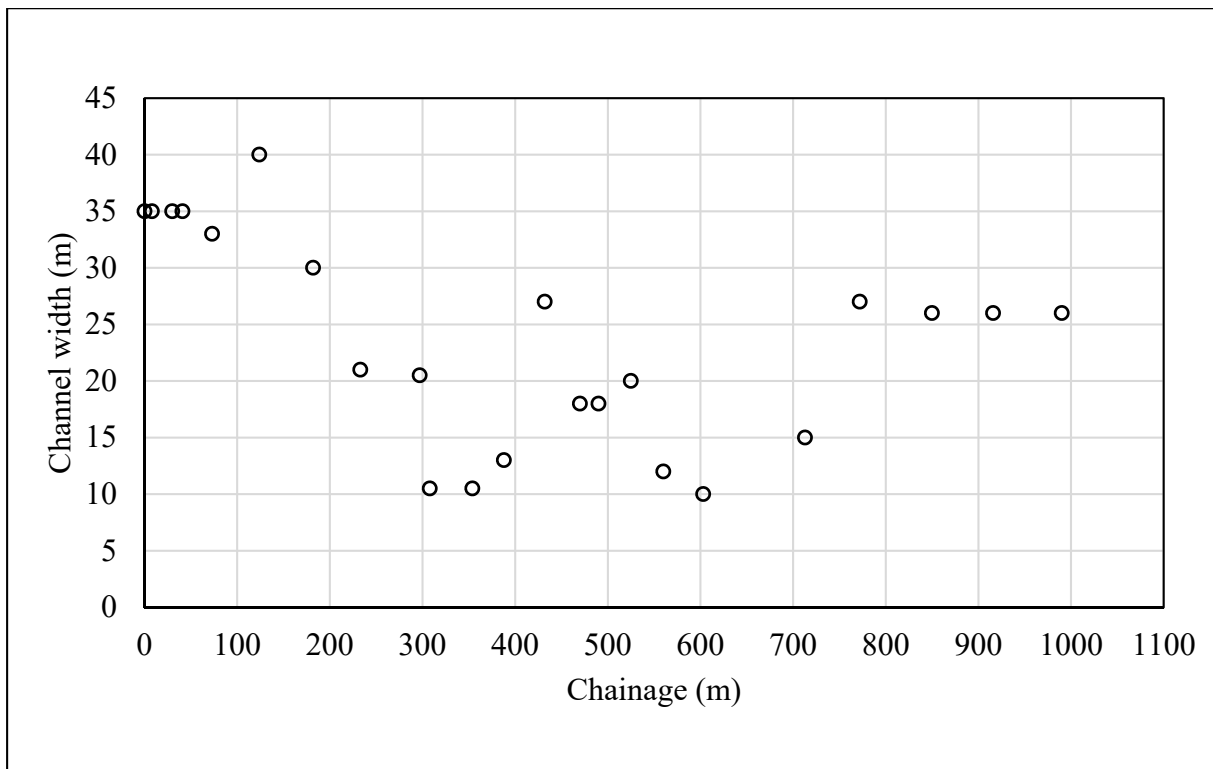


**Figure 4.7 Channel Width Used in Validation between 2d-DMM and DAN-W**

Results indicate that the total entrained volume and run-out distance of the debris are consistent between 2d-DMM (Version 3.0) and DAN-W (Table 4.3, Figure 4.8).

**Table 4.3 Comparison between 2d-DMM and DAN-W Results for Channel of Variable Width**

Program	2d-DMM	DAN-W
Total volume entrained	1719 m <sup>3</sup>	1819 m <sup>3</sup>
Run-out distance	870 m	876 m

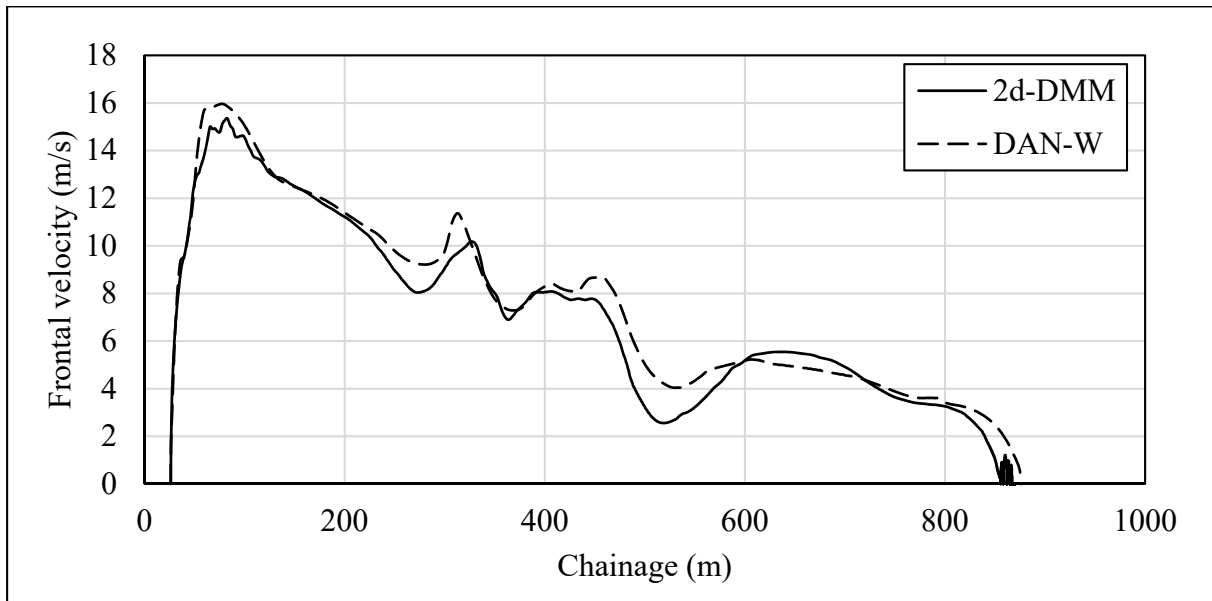


**Figure 4.8 Velocity Profile from 2d-DMM and DAN-W**

### 4.3 Simulation of Yu Tung Road Debris Flow

The new version of 2dDMM has been used to simulate the Yu Tung Road debris flow. The debris flows, initiated by the 7 June 2008 extreme rainstorm, involved a substantial amount of entrainment. In order to validate the new entrainment algorithm embedded in 2dDMM (Version 3.0), the input values of the entrainment depth follow those documented in the detailed landslide field mapping. The width of the landslide trail recorded by the landslide mapping was also adopted in the simulation. The apparent basal friction angle  $\phi_a$  and the Voellmy coefficient  $\xi$  were taken as  $8^\circ$  and  $500 \text{ m/s}^2$  respectively, following results of previous back analysis by Kwan et al. (2011).

The Yu Tung Road event had a source volume of  $2,352 \text{ m}^3$  and a debris run-out path of about 590 m (Hon & Yip, 2008; AECOM, 2012). The entrainment depths along different channel sections as calculated from the mapping record are shown in Table 4.4.

**Table 4.4 Entrainment Depths as Determined from Mapping Record (Sheet 1 of 2)**

Chainage (m)	Gradient ( $^\circ$ )	Trail Width (m)	Erosion ( $\text{m}^3$ )	Entrainment Depth (m)
0-40	35	32.5	2502	-(Source area)
40-55	35	32.5	73	0.18
55-65	25	20	40	0.22
65-90	15	11.8	90	0.32

**Table 4.4 Entrainment Depths as Determined from Mapping Record (Sheet 2 of 2)**

Chainage (m)	Gradient (°)	Trail Width (m)	Erosion (m <sup>3</sup> )	Entrainment Depth (m)
90-105	25	14.2	65	0.34
105-125	25	10	95	0.52
125-140	25	11.4	65	0.42
140-150	15	9.4	45	0.50
150-175	30	12.1	130	0.50
175-180	20	8.6	30	0.74
180-200	10	11	90	0.42
200-220	10	8	55	0.35
220-230	15	10	30	0.31
230-255	20	10	80	0.34
255-270	20	10.7	60	0.40
270-285	20	11.7	70	0.42
285-300	20	11.3	45	0.28
300-310	20	10	40	0.43
310-330	20	12.3	85	0.37
330-340	20	15	40	0.28
340-390	20	11.8	85	0.15
390-415	20	11.4	90	0.34
415-435	25	8	85	0.59
435-455	60	9.7	75	0.77
455-470	20	11	25	0.16
470-510	25	14	110	0.22
510-545	20	16	70	0.13

From field geological mapping, the total volume of debris entrained along the trail was estimated at 1,768 m<sup>3</sup>. A similar entrainment volume of 1,814 m<sup>3</sup> was calculated by 2d-DMM. The calculated velocity profile is also broadly consistent with that determined from super-elevation data obtained in the field (Figure 4.9).

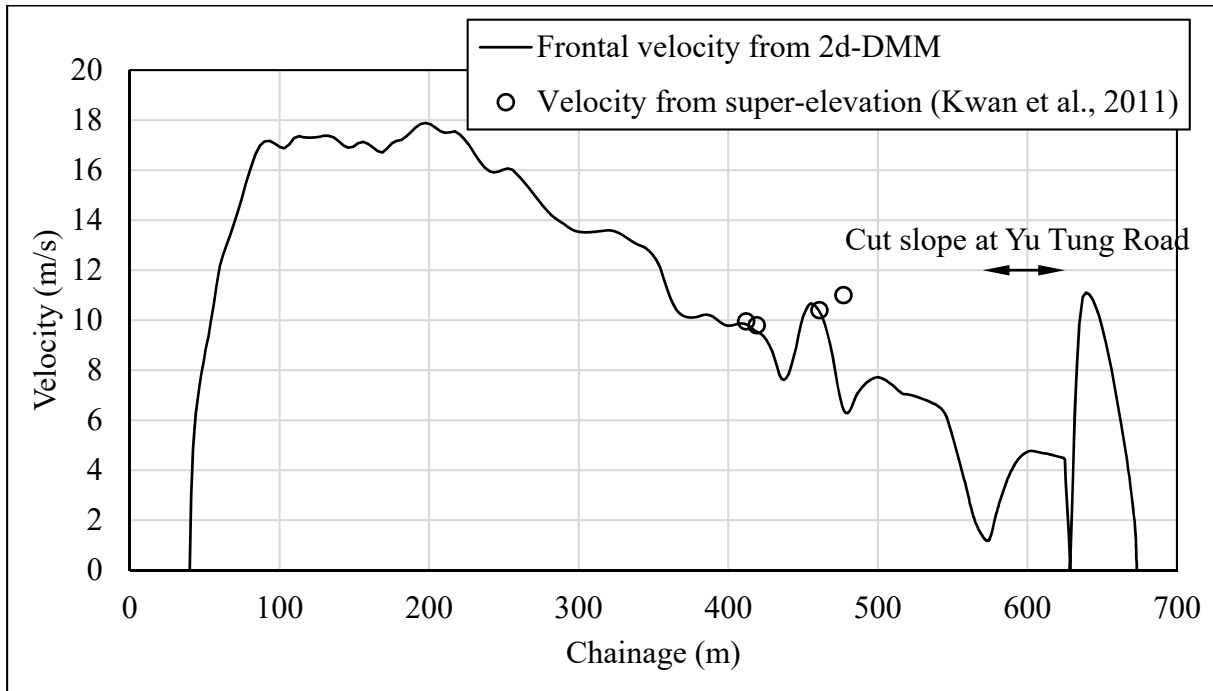


**Figure 4.9 Debris Velocity along Yu Tung Road Debris Flow**

## 5 Entrainment Depth of Debris Flow Events in Hong Kong

As part of the present study, entrainment depths of six massive debris flow events which occurred during the 7 June 2008 rainstorm have been reviewed. Those events are Shek Pik “1”, Shek Pik “2”, Shek Pik “4”, Yu Tung Road, Shek Mun Kap and Sunset Peak “1”. In many of these events, the entrainment volume is over 10 times the landslide source volume, and the areas of the catchments in which they occurred are large, ranging from 10 ha to 70 ha. The locations and a summary of the events are given in Figure 5.1 and Table 5.1. This review serves to present the range of entrainment depths in notable historical debris flows with high mobility and large entrainment volume for reference.

Figure 5.2 shows the distribution of entrainment depth within each mapping section in the six debris flows being considered. It may be observed that the majority of the entrainment depth is below 1 m, with an average of 0.48 m.

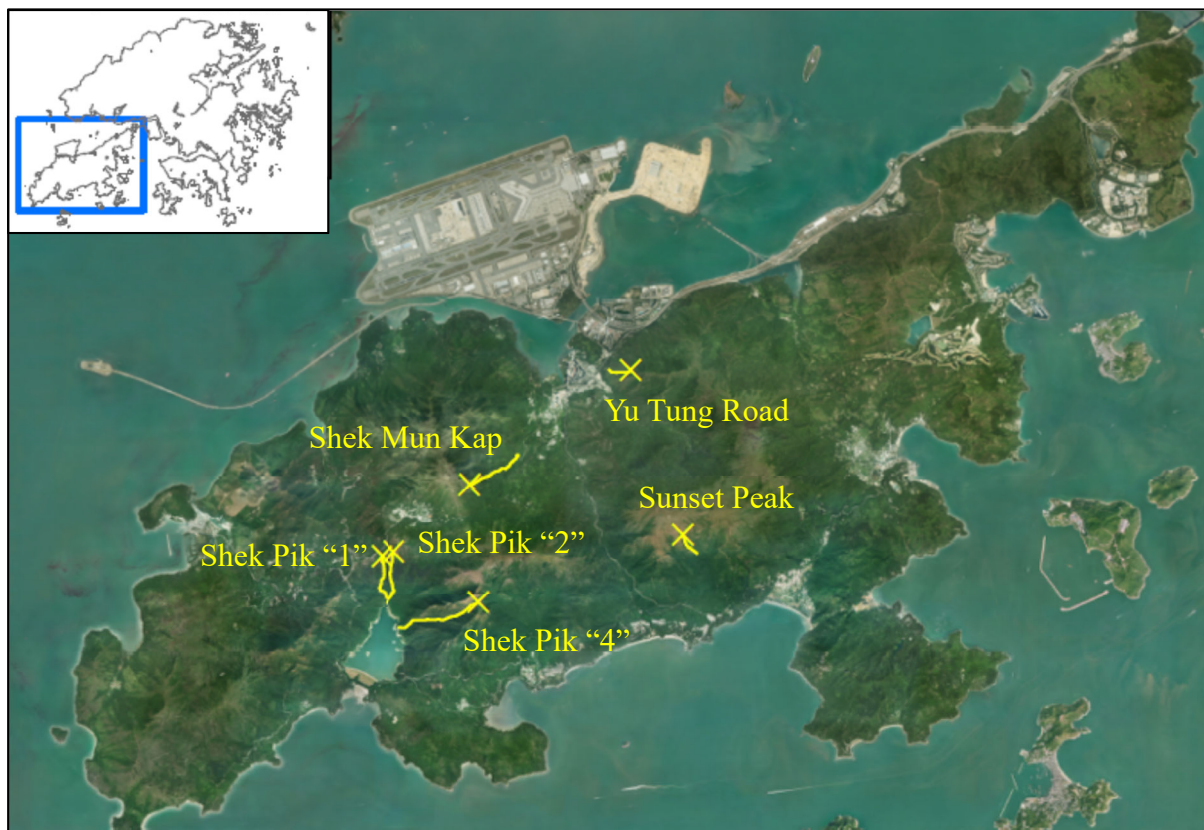


**Figure 5.1 Locations of Debris Flow Events Considered**

**Table 5.1 Debris Flow Events with Greatest Entrained Volume under 2015 Study**

Event	Source Volume (m <sup>3</sup> )	Plan Distance of Landslide Trail (m)	Volume Entrained along Trail (m <sup>3</sup> )	Reference
Shek Pik "2"	1000	1077	11908	LS08-0256 (McMackin & Dee, 2008a)
Shek Pik "1"	324	1023	7101	LS08-0257 (McMackin & Dee, 2008b)
Shek Pik "4"	150	1757	5435	LS08-0260 (Parry et al., 2008)
Yu Tung Road	2352	589	1768	LS08-241 (Hon & Yip, 2008)
Shek Mun Kap	257	1019	2324	LS08-0252 (Leung et al., 2008)
Sunset Peak "1"	220	472	2360	LS08-1136 (Roberts & Ward, 2008)



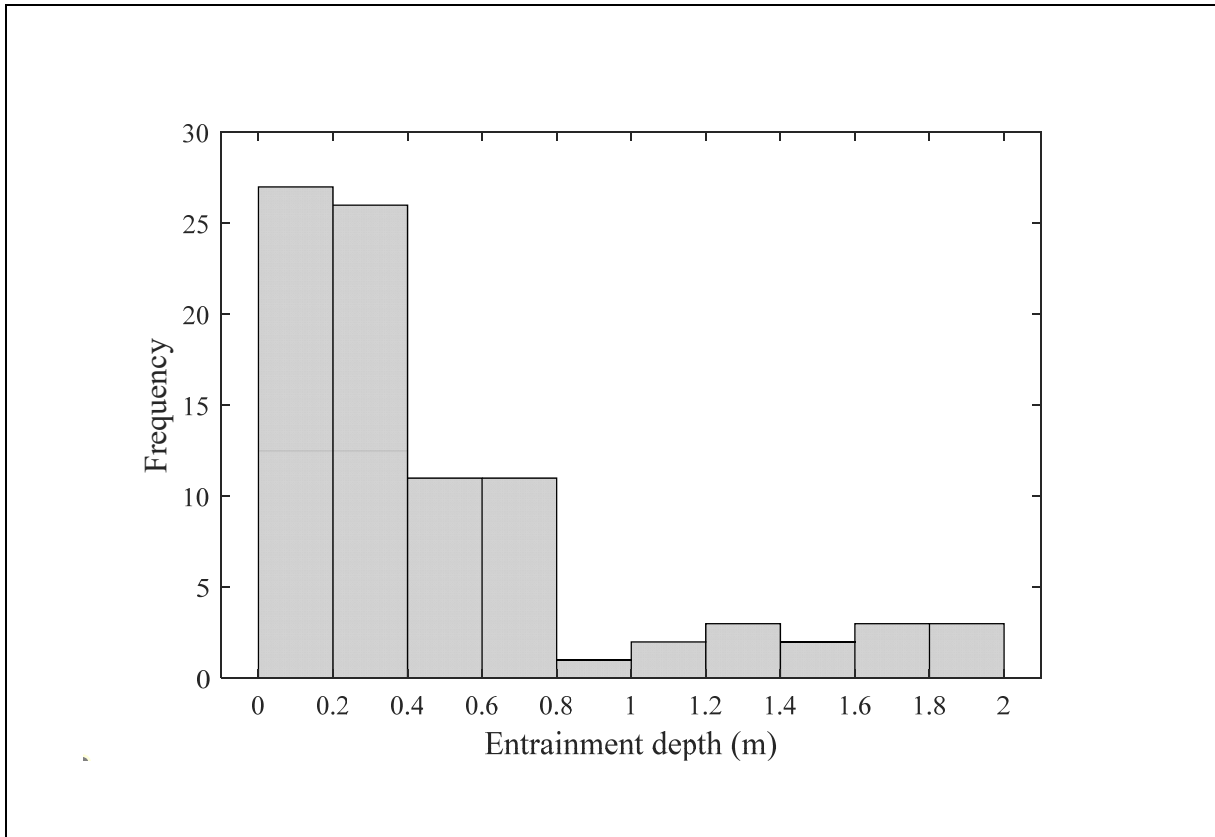


**Figure 5.2 Distribution of Entrainment Depth in Selected Debris Flow Events**

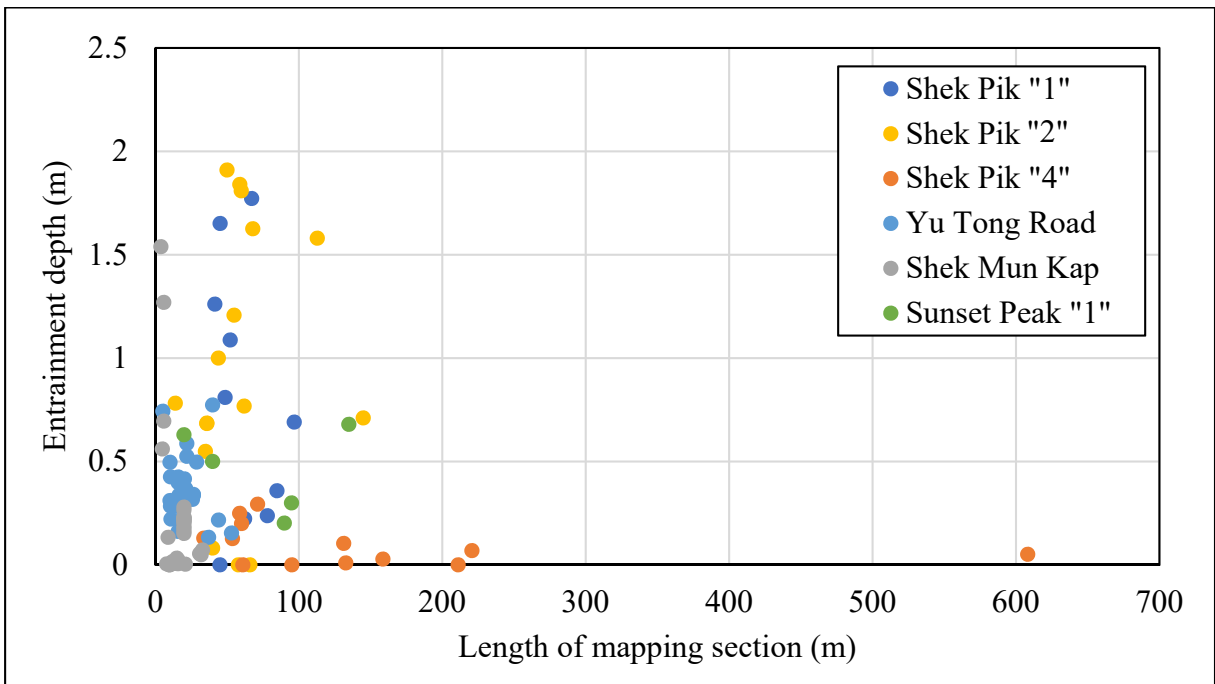


**Figure 5.3 Distribution of Entrainment Depth with Length of Mapping Section**

The distribution may be influenced by the artificial delineation of each debris trail into chainage sections during the mapping exercises. Fine delineation (shorter mapping sections) in a debris flow may cause an over-representation of the particular entrainment depths within that event; conversely, long mapping sections may cause under-representation. Figure 5.3 shows the distribution of the lengths of mapping sections in each debris flow event. The average length of each debris trail mapping section is about 40 m. Relatively longer mapping sections were used in the Shek Pik "4" event but the distribution in Figure 5.2 has not been unduly skewed.

The greatest entrainment depth of 1.9 m occurred in the Shek Pik "2" debris flow between CH. 422 m and CH. 472 m.

It is observed that the entrainment depth decreases with the gradient of the drainage channel in general (Figure 5.4). Steeper channel sections may be less likely to contain loose, easily entrainable material than more gentle channels. Nevertheless, the thickness of entrainable material is specific to each individual flow path and Figure 5.4 should not be used as general guidance on the entrainment depth as a generalised function of slope gradient.

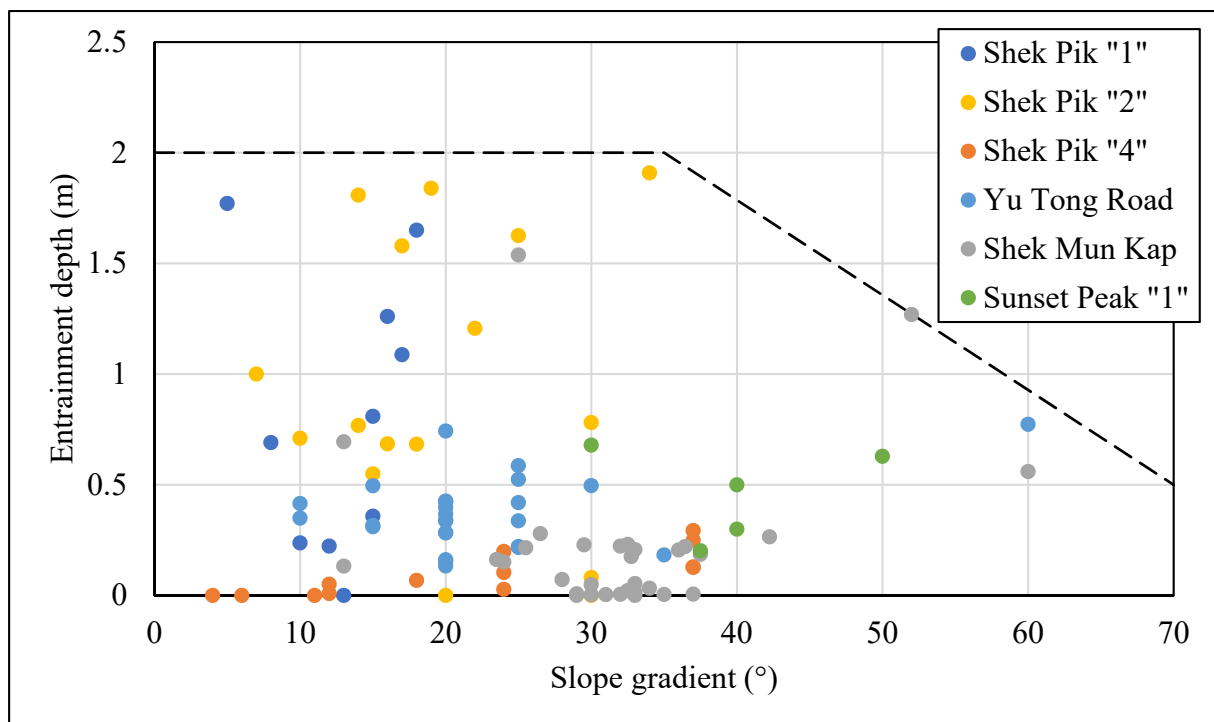


**Figure 5.4 Distribution of Entrainment Depth with Slope Gradient**

GEO (2011) identified large catchments, long flow paths and large number of tributaries feeding into a major drainage line as adverse site settings which may give rise to the development of sizeable debris flows with large amounts of entrainable materials and high mobility. In Figures 5.5 to 5.7, an attempt is made to investigate the possible influence of the drainage characteristics of the natural hillside catchment on the entrainment depth. In these figures, the range and weighted mean (see dots in the figures) of entrainment depths are shown

for each event. The weighted means were obtained by multiplying the entrainment depth in each channel section (as delineated artificially during geological mapping) by the length of the channel section.

It is observed that the catchment size by itself may not give an indication of the entrainment potential in a catchment (Figure 5.5). A larger catchment area does not necessarily indicate greater tendency for surface water to concentrate.

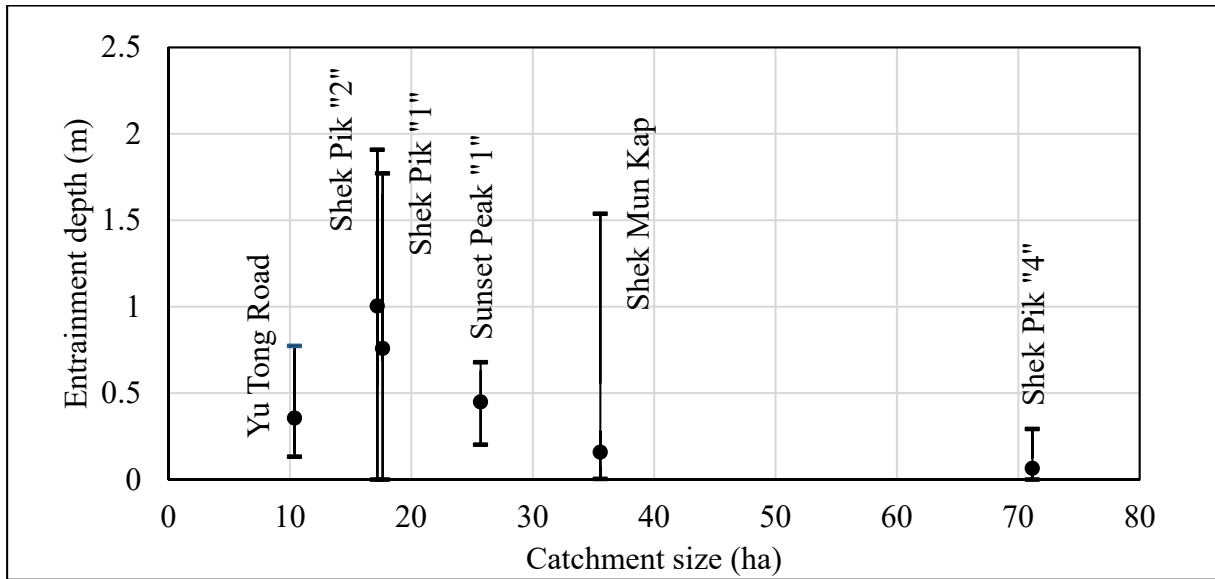


**Figure 5.5 Distribution of Entrainment Depth with Catchment Size**

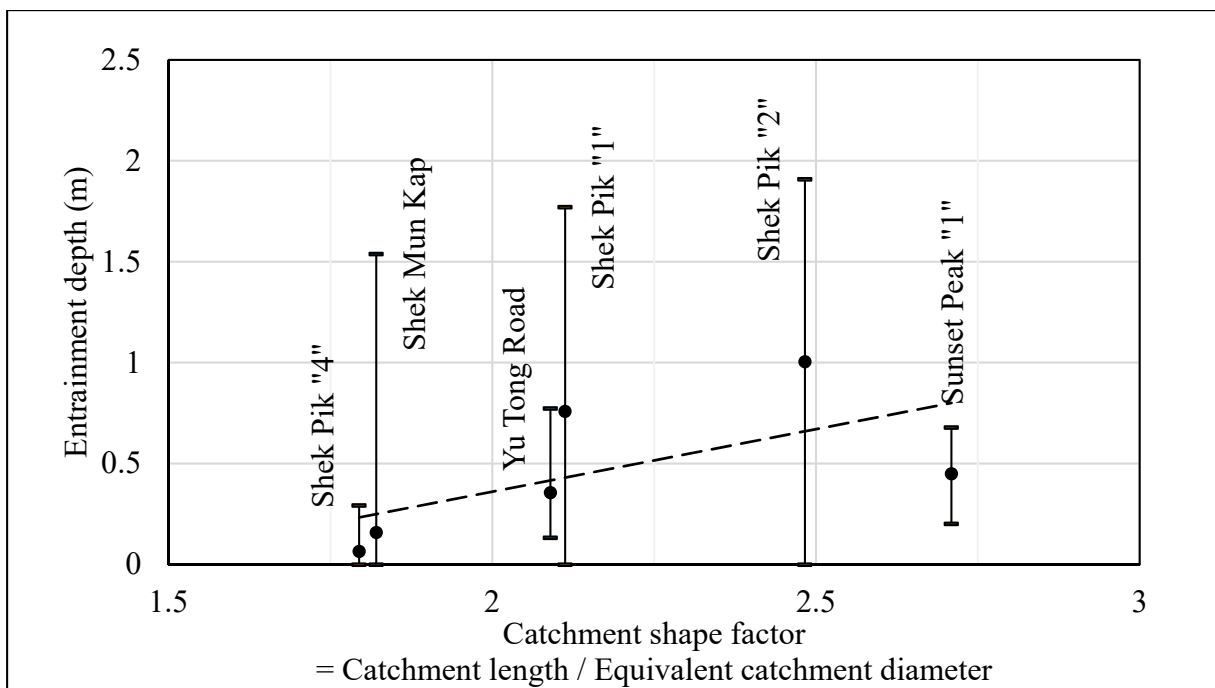


**Figure 5.6 Distribution of Entrainment Depth with Catchment Shape**

In Figure 5.6, the distribution of entrainment depth is plotted against the catchment shape. The catchment shape is defined as the ratio between the catchment length and an equivalent catchment diameter, which is the diameter of a circle with the same plan area as the catchment. A larger catchment shape factor is an indication of a more elongated catchment, and potentially greater concentration of surface water flow along the main drainage line, if any. Amongst the debris flows investigated, the entrainment depth appears to increase with the catchment shape factor.

In Figure 5.7, the distribution of entrainment depth is plotted against the drainage density. The drainage density is defined as the ratio between the total length of prominent drainage lines within the catchment and the catchment area. A larger drainage density is an indication of greater tendency for surface water to flow across longer distances before infiltrating into the ground. Amongst the debris flows investigated, the entrainment depth appears to show a positive correlation with drainage density.

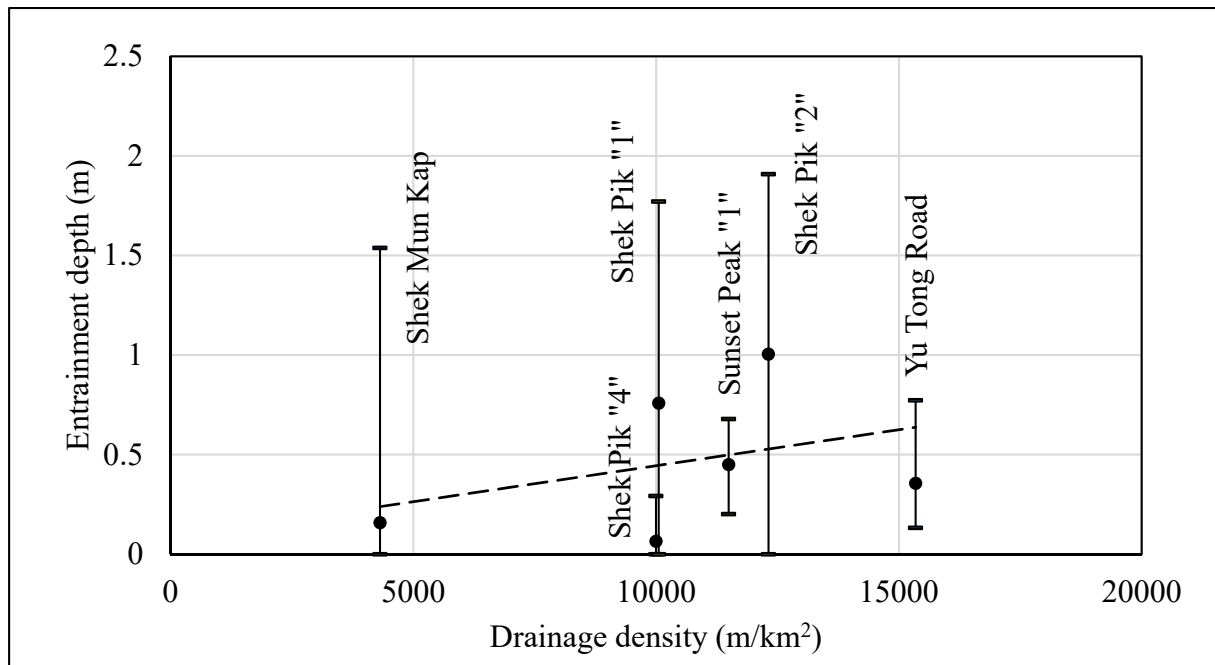


**Figure 5.7 Distribution of Entrainment Depth with Drainage Density**

Nevertheless, the probable trends, associated with the weighted average entrainment depth and the drainage characteristics parameters of the natural hillside catchment observed in Figure 5.6 and Figure 5.7, are not conclusive. The entrainment depth along the run-out path lies in a rather wide range. Other factors, e.g. rheology of the debris flow, erodibility of the regolith in drainage line, abundance of deposit of previous landslides, are essential in determining the amount of entrainment that could occur. When determining the design entrainment rates for the purpose of natural terrain hazard study, a holistic approach with due consideration of the entrainment rates in relevant previous landslide events, if any, should be adopted.

## 6 Conclusion

Enhancement has been made to the debris mobility run-out code 2d-DMM in terms of the modelling of entrainment. The code has been validated against DAN-W and a high mobility debris flow event in June 2008.

A preliminary review of the entrainment depth of notable debris flow events which occurred in June 2008 shows that the entrainment depth may decrease with channel gradient but increase with the concentration of surface water. However, the correlations are not conclusive and should not be taken as generalised relationships in design practice.

## 7 References

- AECOM (2012). *Detailed Study of the 7 June 2008 Landslides on the Hillside above Yu Tung Road, Tung Chung (GEO Report No. 271)*. Geotechnical Engineering Office, Hong Kong, 124 p.
- Ayotte, D., & Hungr, O. (1998). *Runout Analysis of Debris Flow and Debris Avalanches in Hong Kong – A Report for the Geotechnical Engineering Office, Hong Kong*. University of British Columbia, Canada, 90 p.
- Cuomo, S., Pastor, M., Cascini, L., & Castorino, G.C. (2014). Interplay of rheology and entrainment in debris avalanches: a numerical study. *Canadian Geotechnical Journal*, Volume 51, No. 11, pp. 1318-1330.
- Cuomo, S. (2020). Modelling of flowslides and debris avalanches in natural and engineered slopes: a review. *Geoenvironmental Disasters*, Volume 7, No. 1, pp. 1-25.
- GEO (2011). *Guidelines on the Assessment of Debris Mobility for Channelised Debris Flows (GEO Technical Guidance Note No. 29)*. Geotechnical Engineering Office, Hong Kong, 6 p.
- GEO (2012). *Guidelines on Assessment of Debris Mobility for Open Hillslope Failures (GEO Technical Guidance Note No. 34)*. Geotechnical Engineering Office, Hong Kong, 16 p.
- GEO (2013). *Guidelines on the Assessment of Debris Mobility for Failures within Topographic Depression Catchments (GEO Technical Guidance Note No. 38)*. Geotechnical Engineering Office, Hong Kong, 8 p.
- GEO (2015). *User Manual For Computer Program “2d-DMM – Two-dimensional Debris Mobility Model (Version 2.0)”*. Geotechnical Engineering Office, Hong Kong, 31 p.
- Hon, E. & Yip, E. (2008). *Landslide Mapping Report LS08-241*. Geotechnical Engineering Office, Hong Kong, 72 p.
- Hungr, O. (1995). A model for the runout analysis of rapid flow slides, debris flows, and avalanches. *Canadian Geotechnical Journal*, Volume 32, No. 4, pp. 610-623.

- Hungr, O. (1998). *Mobility of Landslides in Hong Kong: Pilot Analysis Using a Numerical Model – A Report for the Geotechnical Engineering Office, Hong Kong*. O. Hungr Geotechnical Research Inc., Canada, 52 p.
- Hungr, O. (2010). *User's Manual, DAN-W Release 10 Dynamic Analysis of Landslides*. O. Hungr Geotechnical Research Inc., Canada, 58 p.
- Hungr, O. & Evans, S.G. (1997). A dynamic model for landslides with changing mass. *Proceedings of the International Symposium on Engineering Geology and the Environment*, Volume 1, pp. 719-724.
- Iverson, R. (2012). Elementary theory of bed-sediment entrainment by debris flows and avalanches. *Journal of Geophysical Research*, Volume 117, No. F3, pp. 1-17.
- Iverson, R.M. & Ouyang, C. (2015). Entrainment of bed material by Earth-surface mass flows: Review and reformulation of depth-integrated theory. *Review of Geophysics*, Volume 53, No. 1, pp. 27-58.
- Kong, Y., Zhao, J.D. and Li, X.Y. (2018). Coupled CDF/DEM modelling of multiphase debris flow over a natural erodible terrain: the Yu Tung Road case. *Proceedings of the Second JTCl Workshop on Triggering and Propagation of Rapid Flow-like Landslides*, Hong Kong, pp. 197-200.
- Kwan, J.S.H., Hui, T.H.H. & Ho, K.K.S. (2011). Modelling of the motion of mobile debris flows in Hong Kong. *Proceedings of the 2<sup>nd</sup> World Landslide Forum*, Rome, 3-7 October 2011.
- Kwan, J.S.H. & Sun, H.W. (2006). An improved landslide mobility model. *Canadian Geotechnical Journal*, Volume 43, No. 5, pp. 531-539.
- Kwan, J.S.H. & Sun, H.W. (2007). Benchmarking exercise on landslide mobility modelling – runout analyses using 3dDMM. *Proceedings of the International Forum on Landslide Disaster Management, Hong Kong, Geotechnical Division, Hong Kong Institution of Engineers*, Hong Kong, Volume II, pp. 945-966.
- Kwan, J.S.H., Sze, E.H.Y., Lam, C., Law, R.P.H. & Koo, R.C.H. (2021). Development and applications of debris mobility models in Hong Kong. *Proceedings of the Institution of Civil Engineers – Geotechnical Engineering*, Volume 174, pp. 593-610.
- Law, R.P.H. & Ko, F.W.Y. (2015). *Validation of Geotechnical Computer Program “2d-DMM (Version 2.0)” (GEO Technical Note No. TN 1/2015)*. Geotechnical Engineering Office, Hong Kong, 97 p.
- Law, R.P.H., Kwan, J.S.H., Ko, F.W.Y. & Sun, H.W. (2017). Three-dimensional debris mobility modelling coupling smoothed particle hydrodynamics and ArcGIS. *Proceedings of the 19<sup>th</sup> International Conference on Soil Mechanics and Geotechnical Engineering (Seoul)*, South Korea, pp. 3501-3504.

- Leung, A.W.K., Law, Y.M.S., Lau, R. (2008). *Landslide Mapping Report LS08-0252*. Geotechnical Engineering Office, Hong Kong, 53 p.
- McDougall, S. & Hungr, O. (2005). Dynamic modelling of entrainment in rapid landslides. *Canadian Geotechnical Journal*, Volume 42, No. 5, pp. 1437-1448.
- McMackin, M. & Dee, S. (2008a). *Landslide Mapping Report LS08-0256*. Geotechnical Engineering Office, Hong Kong, 35 p.
- McMackin, M. & Dee, S. (2008b). *Landslide Mapping Report LS08-0257*. Geotechnical Engineering Office, Hong Kong, 35 p.
- Parry, S., Hart, J. & Moore, A. (2008). *Landslide Mapping Report LS08-0260*. Geotechnical Engineering Office, Hong Kong, 25 p.
- Perla, R., Cheng, T. & McClung, D. (1980). A two-parameter model of snow-avalanche motion. *Journal of Glaciology*, Volume 26, No. 94, pp. 197-207.
- Pirulli, M., Leonardi, A., & Scavia, C. (2018). Comparison of depth-averaged and full-3D model for the benchmarking exercise on landslide runout. *Proceedings of the Second JTCl Workshop on Triggering and Propagation of Rapid Flow-like Landslides*, Hong Kong, pp. 240-253.
- Pirulli, M. & Pastor, M. (2012). Numerical study on the entrainment of bed material into rapid landslides. *Géotechnique*, Volume 62, No. 11, pp. 959-972.
- Roberts, P.A. & Ward, P.N. (2008). *Landslide Mapping Report LS08-1136*. Geotechnical Engineering Office, Hong Kong, 35 p.
- Shen, W., Li, T., Li, P. & Guo, J. (2018). A modified finite difference model for the modeling of flowslides. *Landslides*, Volume 15, No. 8, pp. 1577-1593.
- Takahashi, T. (1991). *Debris flow*. IAHR-AIRH Monograph series, A. A. Balkema, 165 p.

## GEO PUBLICATIONS AND ORDERING INFORMATION

### 土力工程處刊物及訂購資料

An up-to-date full list of GEO publications can be found at the CEDD Website <http://www.cedd.gov.hk> on the Internet under "Publications". The following GEO publications can also be downloaded from the CEDD Website:

- i. Manuals, Guides and Specifications
- ii. GEO technical guidance notes
- iii. GEO reports
- iv. Geotechnical area studies programme
- v. Geological survey memoirs
- vi. Geological survey sheet reports

**Copies of some GEO publications (except geological maps and other publications which are free of charge) can be purchased either by:**

#### Writing to

Publications Sales Unit,  
Information Services Department,  
Room 626, 6th Floor,  
North Point Government Offices,  
333 Java Road, North Point, Hong Kong.

#### or

- Calling the Publications Sales Section of Information Services Department (ISD) at (852) 2537 1910
- Visiting the online Government Bookstore at <http://www.bookstore.gov.hk>
- Downloading the order form from the ISD website at <http://www.isd.gov.hk> and submitting the order online or by fax to (852) 2523 7195
- Placing order with ISD by e-mail at [puborder@isd.gov.hk](mailto:puborder@isd.gov.hk)

**1:100 000, 1:20 000 and 1:5 000 geological maps can be purchased from:**

Map Publications Centre/HK,  
Survey & Mapping Office, Lands Department,  
23th Floor, North Point Government Offices,  
333 Java Road, North Point, Hong Kong.  
Tel: (852) 2231 3187  
Fax: (852) 2116 0774

**Any enquires on GEO publications should be directed to:**

Chief Geotechnical Engineer/Planning and Development,  
Geotechnical Engineering Office,  
Civil Engineering and Development Department,  
Civil Engineering and Development Building,  
101 Princess Margaret Road,  
Homantin, Kowloon, Hong Kong.  
Tel: (852) 2762 5351  
Fax: (852) 2714 0275  
E-mail: [ivanli@cedd.gov.hk](mailto:ivanli@cedd.gov.hk)

詳盡及最新的土力工程處刊物目錄，已登載於土木工程拓展署的互聯網網頁<http://www.cedd.gov.hk>的“刊物”版面之內。以下的土力工程處刊物亦可於該網頁下載：

- i. 指南、指引及規格
- ii. 土力工程處技術指引
- iii. 土力工程處報告
- iv. 岩土工程地區研究計劃
- v. 地質研究報告
- vi. 地質調查圖表報告

**讀者可採用以下方法購買部分土力工程處刊物(地質圖及免費刊物除外):**

#### 書面訂購

香港北角渣華道333號  
北角政府合署6樓626室  
政府新聞處  
刊物銷售組

#### 或

- 致電政府新聞處刊物銷售小組訂購 (電話：(852) 2537 1910)
- 進入網上「政府書店」選購，網址為 <http://www.bookstore.gov.hk>
- 透過政府新聞處的網站 (<http://www.isd.gov.hk>) 於網上遞交訂購表格，或將表格傳真至刊物銷售小組 (傳真：(852) 2523 7195)
- 以電郵方式訂購 (電郵地址：[puborder@isd.gov.hk](mailto:puborder@isd.gov.hk))

**讀者可於下列地點購買1:100 000、1:20 000及1:5 000地質圖：**

香港北角渣華道333號  
北角政府合署23樓  
地政總署測繪處  
電話: (852) 2231 3187  
傳真: (852) 2116 0774

**如對本處刊物有任何查詢，請致函：**

香港九龍何文田公主道101號  
土木工程拓展署大樓  
土木工程拓展署  
土力工程處  
規劃及拓展部總土力工程師  
電話: (852) 2762 5351  
傳真: (852) 2714 0275  
電子郵件: [ivanli@cedd.gov.hk](mailto:ivanli@cedd.gov.hk)